THE JOURNAL OF PHYSICAL CHEMISTRY A

ARTICLE

pubs.acs.org/JPCA

Photophysical and Electronic Properties of Five PCBM-like C_{60} Derivatives: Spectral and Quantum Chemical View

Huan Wang,[†,§] Youjun He,[‡,§] Yongfang Li,[‡,§] and Hongmei Su*[,†,§]

[†]State Key Laboratory of Molecular Reaction Dynamics, [‡]The CAS Key Laboratory of Organic Solids, and [§]Beijing National Laboratory for Molecular Sciences (BNLMS), Institute of Chemistry, Chinese Academy of Sciences, Beijing 100190, People's Republic of China

ABSTRACT: By means of transient UV−visible absorption spectra/fluorescence spectra, combined with electronic structure calculations, the present work focuses on characterizing the photophysical and electronic properties of five PCBM-like C_{60} derivatives (F1, F2, F3, F4, and F5) and understanding how these properties are expected to affect the photovoltaic performance of polymer solar cells (PSCs) with those molecules as acceptors. Spectral data reveal that the fluorescence quantum yields (Φ_F) are enhanced and the triplet quantum yields (Φ_T) are lowered for the five PCBM-like C_{60} derivatives as compared to those of the pristine C_{60}, suggesting that functionalization of a C═C double bond perturbs the fullerene's π-system and breaks the I_h symmetry of pristine C_{60}, which results in modifications of photophysical properties of the fullerene derivatives. PBEPBE/6-311G(d,p)//PBEPBE/6-31G(d) level of electronic structure calculations yields the HOMO−LUMO gaps and LUMO energies, showing that the electron-withdrawing effect induced by the side chain functional groups perturbs LUMO energies, from which different open circuit voltages V_{oc} are resulted. The predicted V_{oc} from our calculation agrees with previous experiment results. Basically, we found that functionalization of a C═C double bond sustains the fullerene structure and its electron affinitive properties. Adducted side chains contribute to adjust the HOMO−LUMO gap and LUMO levels of the acceptors to improve open circuit voltage. The results could provide fundamental insights for understanding how structural modifications influence the photovoltaic performance, which paves a way for guiding the synthesis of new fullerene derivatives with improved performance in polymer solar cells.

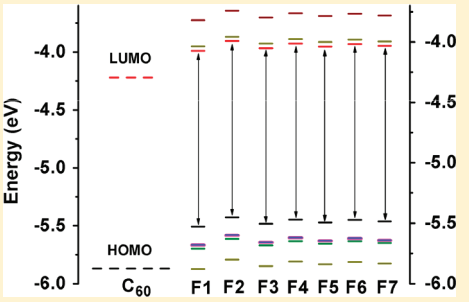

1. INTRODUCTION

Organic solar cells, especially the solution-processed polymer/fullerene-based bulk heterojunction (BHJ) polymer solar cells (PSCs), have attracted much interest in the past two decades because they hold the potential to be low-cost, large-area, flexibile, lightweight solar energy conversion devices.[1−7] Because of the high electron affinity and superior ability to transport charge effectively, fullerenes can be used as potential acceptor components for photovoltaic devices.[8] However, because of the low solubility, fullerenes are incompatible with solution-based processing. To improve solubility, many works are devoted to modifying fullerenes by adding functional groups to the fullerene core, among which the higher soluble derivative [6,6]-phenyl-C_{61}-butyric acid methyl ester (PCBM) was first synthesized by Hummelen[9] and used to replace C_{60} as the acceptor.[1] Since then, considerable progress has been made in the PSCs field, which have been detailed in several excellent review articles.[10−13]

A well-studied system is the solution processable P3HT/PCBM BHJ blends,[14] with power conversion efficiency (PCE) reported to be about 4%.[15−17] To further improve the photovoltaic performance, many fullerene derivatives were synthesized with mono-[18−24] or multiple-functional groups,[18,22,25−27] or electron-donor groups on the phenyl ring,[28,29] or replacing the phenyl ring instead.[24,27,30] In addition, other novel fullerene derivatives such as indene-C_{60} bisadduct[31,32] and endohedral fullerenes[33,34] were synthesized. The PSCs based on some of these derivatives were reported to have PCE approaching 5% or even higher,[25,31−33] but most of them showed results poorer than or merely comparable to that of PCBM. Therefore, PCBM is still considered to be an advanced acceptor material and is used typically in polymer solar cells.

Recently, we have designed and synthesized a series of PCBM-like C_{60} derivatives, F1, F2, F3, F4, and F5 (Scheme 1), by changing the butyl carbon chain length of PCBM (F2) from 3 to 7 carbon atoms, respectively, to investigate the effect of the carbon chain length of PCBM on the photovoltaic performance of these PCBM derivatives in the PSCs with P3HT as donor and F1−F5 as acceptor.[35] The PSCs with F1, F2, or F4 as the acceptor were found to display higher photovoltaic performance with PCE above 3.5%, while those with F3 or F5 as acceptors showed a relatively lower PCE below 3.0%. The different performances among the five PCBM-like fullerene derivatives were explained mainly on the basis of their electron mobilities and morphology properties.

As compared to the well-characterized photovoltaic performance, the photophysical and electronic properties of these PCBM derivatives remain unknown to a large extent, while these

Received: September 4, 2011
Revised: October 29, 2011
Published: November 30, 2011

Scheme 1. Structures of Five PCBM-like Fullerene Derivatives. F1, F2, F3, F4, F5

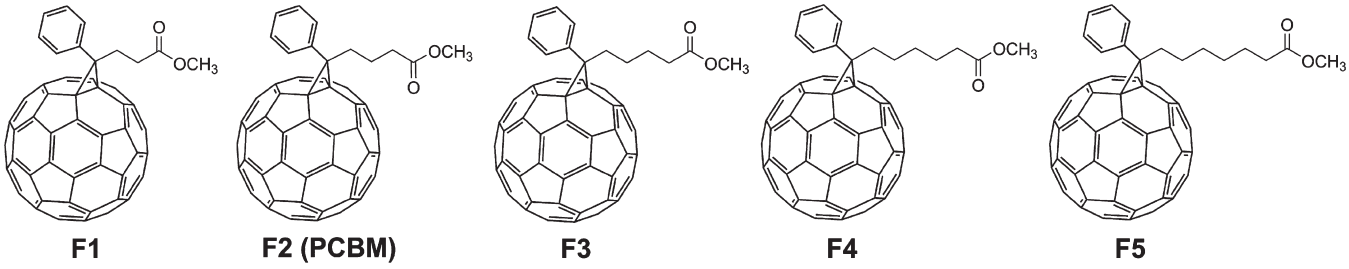

properties are crucial to understanding the complex exciton dissociation processes at the donor−acceptor interface that ultimately affect the photovoltaic performance. For example, in bis-dicyanovinyl-olgothiophenes/fullerene blends, it has been observed that, for certain thiophene oligomer lengths, excitons can efficiently transfer to C_{60}, where the large intersystem crossing leads to the formation of triplet excitons, which then hop back to the donor; such processes do not result in charge separation and constitute a loss mechanism.[36] Obviously, the formation of triplet excitons involved in such a loss mechanism is highly dependent on the photophysical properties of donor and acceptor molecules, among which energy transfer and intersystem crossing play key roles.

The present work will focus on characterizing the photophysical and electronic properties of the five PCBM-like C_{60} derivative molecules (F1, F2, F3, F4, and F5 shown in Scheme 1) and understanding how these properties are expected to affect the photovoltaic performance of PSCs. By measuring the transient UV−visible absorption spectra, transient fluorescence decay, together with the steady-state UV−visible absorption and fluorescence spectra, the photophysical processes of fluorescent emission and intersystem crossing were examined. Because of the symmetry breaking effect of the side chain addition to fullerene core, the fluorescence quantum yields (Φ_F) are enhanced and the triplet quantum yields (Φ_T) are lowered for the five PCBM-like C_{60} derivatives as compared to those of the pristine C_{60}. In addition, the HOMO−LUMO gaps and LUMO energies were calculated by PBEPBE/6-311G(d,p)//PBEPBE/6-31G(d) level of density functional theories, showing that the electron-withdrawing effect induced by the side chain functional groups perturbs LUMO energies of the five fullerene derivatives, from which different open circuit voltages V_{oc} are resulted. The predicted V_{oc} values from our calculations agree with previous experimental results[35] and afford reasonable explanations by revealing the small variation of LUMO energies. By closely examining the variation of photophysical and electronic properties, the results of the current work could provide a fundamental understanding of how structural modifications influence the LUMO levels and the open circuit voltages, which are key factors determining the photovoltaic performance of polymer solar cells.

2. EXPERIMENTAL AND THEORETICAL METHODS

Materials. Five PCBM-like C_{60} derivatives, F1, F2, F3, F4, and F5, were synthesized as described elsewhere.[35] The molecular structures are shown in Scheme 1. These molecules belong to a class of functionalized fullerene derivatives called methanofullerenes, with a cyclopropane ring adducted to a C═C double bond located at a junction of two hexagons of C_{60} core. For F1, F2, F3, F4, and F5, there are two substituents linked to the cyclopropane ring: one is the phenyl and the other is the aliphatic chain. The reference sample, C_{60} (99.5%), was purchased from Aldrich and used as received. HPLC grade of toluene was used as solvent.

Steady-State Spectral Measurements. Absorption spectra were recorded with a UV−vis spectrometer (model U-3010, Hitachi). Fluorescence spectra were measured with a fluorescence spectrometer (F4600, Hitachi). For fluorescence quantum yield measurements, the absorbance of all samples was adjusted to 0.1 in 10 mm path length quartz cuvettes at the excitation wavelength (532 nm).

Laser Flash Photolysis. Nanosecond time-resolved laser flash photolysis setup was described previously.[37] Briefly, the instrument comprises a Edinburgh LP920 spectrometer (Edinburgh Instruments Ltd.) combined with an Nd:YAG laser (Surelite II, Continuum Inc.). The sample was excited by 355 nm laser pulse (1 Hz, fwhm ~7 ns), and a 450 W pulsed xenon lamp was used as analyzing light. A monochromator equipped with a photomultiplier for collecting the spectral range from 300 to 850 nm was used to record transient absorption spectra. The signals from the photomultiplier were displayed and recorded as a function of time on a 100 MHz (1.25 Gs/s sampling rate) oscilloscope (Tektronix, TDS 3012B), and the data were transferred to a personal computer. Samples were freshly prepared for each measurement and were adjusted to an absorbance of about 0.25 in 10 mm path length quartz cuvettes at the laser wavelength used. Data were analyzed by the online software of the LP920 spectrometer. The fitting quality was judged by weighted residuals and a reduced χ^2 value.

Fluorescence Lifetime Measurement. Fluorescence decays were measured using the time-correlated single-photon counting (TCSPC) spectrometer (F900, Edinburgh Instrument). The samples were excited at 442 nm using an 80 ps laser diode (PicoQuant PDL 808). Fluorescence decays were monitored through a monochromator at the emission maxima. The instrumental response function (IRF) of our setup was about 200 ps.

Electronic Structure Calculation. The geometries of C_{60}, F1, F2, F3, F4, and F5 were optimized by density functional theory using the gradient-corrected exchange-correlation functional of Perdew, Burke, and Ernzerhof (PBE),[38] with the standard 6-31G(d) basis set, which has proved to yield reliable results at reasonable computation costs for large carbon structures. All optimized geometries were confirmed with no imaginary frequencies. To obtain a more accurate HOMO−LUMO gap, orbital energies were calculated with higher basis sets at the PBEPBE/6-311G(d,p) level. Calculations were performed with the Gaussian 03 program package.[39]

3. RESULTS AND DISCUSSION

Figure 1a displays the UV−visible absorption spectra of five PCBM-like fullerene derivatives, F1, F2, F3, F4, and F5, in toluene. For comparison, the UV−visible spectrum of C_{60} in toluene is also shown. In the UV range below 350 nm, the five PCBM-like fullerene derivatives and C_{60} exhibit nearly the same absorption bands, which correspond to the strong allowed transition of the fullerene core. In the visible region where the transition is mostly symmetry forbidden for the highly symmetric molecule of C_{60}, the broad absorption bands from 450 to 650 nm in C_{60} slightly blue shift for five PCBM-like fullerene derivatives, together with the appearance of two small distinct peaks at ~430 and ~695 nm. These features are very similar to those reported for several other methanofullerenes,[19−21,40] suggesting that the side chains of the fullerene derivatives perturb only the forbidden transitions of fullerene core in the visible region by breaking the I_h symmetry of the pristine C_{60} molecule, whereas the allowed transitions in the UV region are much less affected.

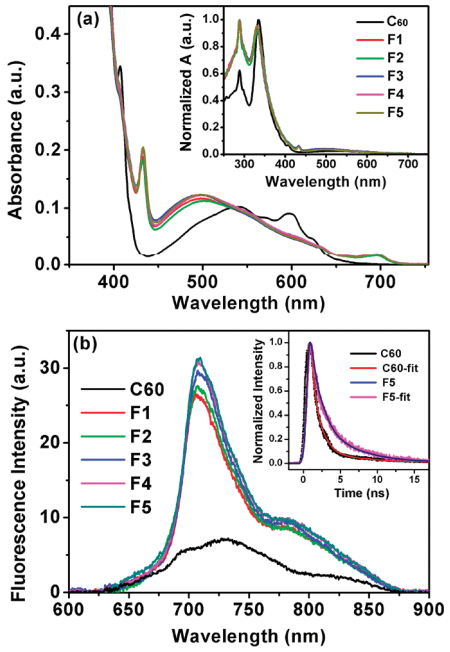

Figure 1. (a) UV−vis absorption spectra of F1, F2, F3, F4, and F5 in toluene collected from 350 to 750 nm, along with the spectra of C_{60} for comparison. Spectral intensities are normalized to the absorbance at 532 nm for all samples (inset: normalized UV−vis absorption spectra for all samples at lower concentration to display the full range spectra without saturation). (b) Fluorescence spectra of C_{60}, F1, F2, F3, F4, and F5 in toluene solution collected from 600 to 900 nm with excitation wavelength at 532 nm (inset: representative fluorescence decay curves and the single exponential fitting).

Figure 1b shows the fluorescence spectra of C_{60} and five fullerene derivatives in toluene solution. The fluorescence spectra of five PCBM-like fullerene derivatives are very similar to each other, showing two peaks at ~708 and ~779 nm. In comparison with C_{60}, the fluorescence intensities of the five fullerene derivatives become larger, and the fluorescence quantum yields (Φ_F) are about 2−3 times higher than that of C_{60}, as shown in Table 1. The enhanced fluorescence intensities and quantum yields are also ascribed to the symmetry breaking effect of side chain addition to the C_{60} core, which strengthens the forbidden transitions from the S_1 to S_0 state to some extent and results in increased emission intensity. On the other hand, no significant differences exist among five PCBM-like fullerene derivatives for their fluorescence spectra, indicating that the increasing of side chain length affects little the transition probabilities from the S_1 to S_0 state.

The fluorescence decays of C_{60} and five fullerene derivatives in toluene solution were measured using standard TCSPC method. The decay curves can be deconvoluted from corresponding instrument response functions (IRF) using a single exponential equation, as shown in Figure 1b, inset. The determined fluorescence lifetimes are listed in Table 1. The fluorescence lifetime of C_{60} (1.18 ns) matches previous reports.[41,42] The five fullerene derivatives possess longer fluorescence lifetimes falling all around 1.4−1.5 ns, indicating their longer-lived excited singlet states than that of C_{60}. Still, no apparent difference exists among the five fullerene derivatives for their fluorescence lifetimes, providing additional evidence that the excited singlet state properties are little affected by the functional groups in different fullerene derivatives.

In parallel to the fluorescent emission, how are other photophysical processes such as intersystem crossing influenced by the side chain addition to the fullerene core? Following nanosecond laser flash photolysis at 355 nm, the transient UV−visible absorption spectra of five fullerene derivatives in toluene solution were measured and shown in Figure 2, along with their comparison C_{60}.

The C_{60} transient spectra in Figure 2a exhibit a typical triplet−triplet absorption band at 750 nm as reported in literature.[43,44] For the five PCBM-like fullerene derivatives, their transient spectra appear very similar to each other, which are featured by maximum absorption at 720 nm as shown from Figure 2b−f. All of the transient absorption bands at 720 nm show first-order decay kinetics (see Figure 2, insets), with a lifetime of several microseconds at deaerated conditions but decreasing to ~300 ns in the presence of O_2. The efficient quenching by dissolved

Table 1. Photophysical Parameters Obtained from Spectral Measurements for F1, F2, F3, F4, and F5, Using C_{60} as Reference

samples	absorption peak/nm (ε_G/M^{-1} cm^{-1})	$\Phi_F{}^a \times 10^{-4}$	τ_F/ ns	T−T peak/ nm	τ_T(deaerated)/ μs	τ_T(air-saturated)/ ns	ε_T/ M^{-1} cm^{-1}	$\Phi_T{}^d$
C_{60}	288(42 232), 335(67 667), 407(4581), 540(1527), 596(1290)	3.2[b]	1.18	750	5.0	302.3	20 200[c]	1
F1	228(44 963), 331(42 953), 432(2604), 502(1582), 694(192)	8.2	1.39	720	5.1	302.7	26 003	0.55
F2	228(43 250), 331(39 675), 433(2412), 502(1512), 695(201)	8.3	1.43	720	3.5	312.7	22 433	0.54
F3	228(47 463), 331(45 059), 433(2893), 498(1818), 695(236)	8.7	1.47	720	2.8	301.3	29 596	0.58
F4	228(44 622), 331(42 437), 433(2438), 498(1547), 695(192)	8.9	1.50	720	3.5	308.7	24 311	0.69
F5	228(46 746), 331(44 622), 433(2639), 499(1625), 696(262)	9.3	1.52	720	3.3	304.9	30 433	0.58

[a] $\Phi^x{}_F = \Phi^{st}{}_F(I^x/I^{st})(A^{st}/A^x)$, Φ_F determined using C_{60} as reference. [b] Data cited from ref 19. [c] Data cited from ref 44. [d] $\Phi^x{}_T = \Phi^{st}{}_T$ $(\Delta\varepsilon_T{}^{st}/\Delta\varepsilon^x{}_T)(\Delta OD^x/\Delta OD^{st})$, Φ_T derived by comparative method using C_{60} as reference.

dx.doi.org/10.1021/jp208520v |J. Phys. Chem. A 2012, 116, 255–262

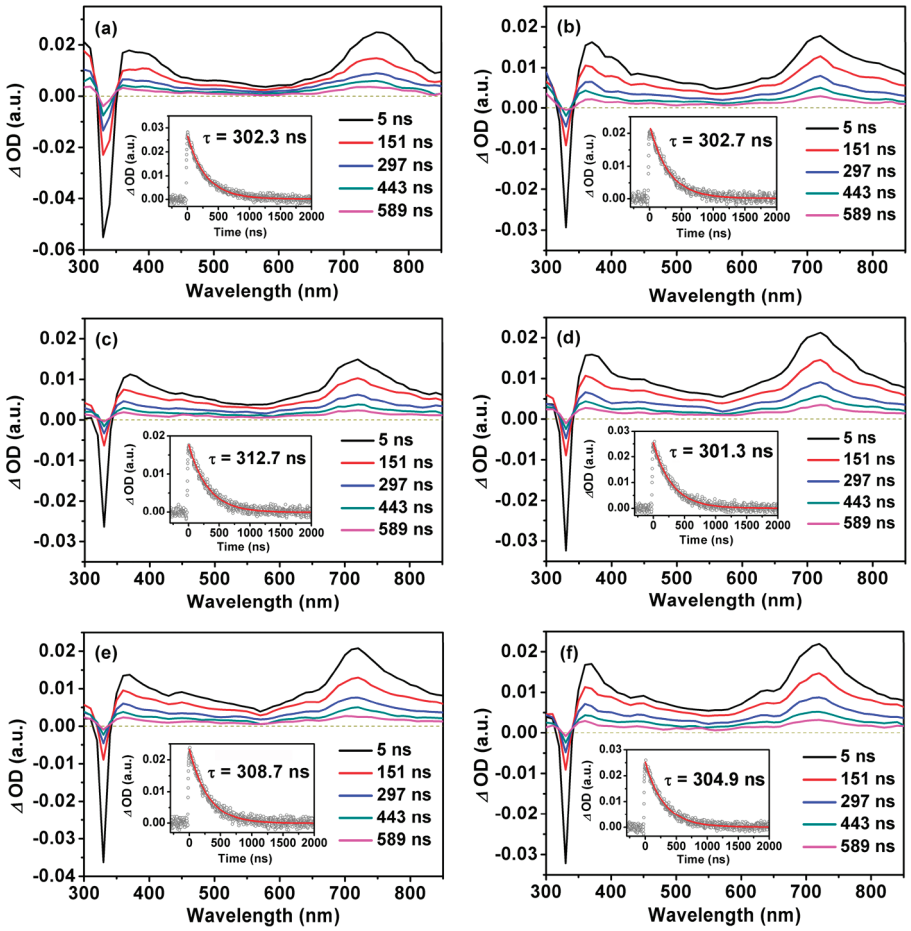

Figure 2. Transient absorption spectra of (a) C_{60}, (b) F1, (c) F2, (d) F3, (e) F4, and (f) F5 at different delay times after laser flash photolysis at 355 nm in toluene solution. Insets show the decay kinetics of transient absorptions at 750 nm for C_{60} and 720 nm for F1−F5.

oxygen confirms the assignment of transient absorption bands at 720 nm to the triplet of PCBM-like fullerene derivatives.

As compared to C_{60}, the transient triplet−triplet absorption bands are blue-shifted by about 30 nm for the five PCBM-like fullerene derivatives, as found in other methanofullerenes.[18,20,21] The addition of functional groups to the C═C double bond converts sp^2-hybridized carbons into sp^3-hybridized ones, resulting in a contraction of π-system to 58 π-electrons as compared to the pristine C_{60} with 60 π-electrons. By lifting of double bonds, such a perturbation to the fullerene's π-system leads to less π-conjugation, and thus blue-shift absorption for triplet−triplet transitions as compared to C_{60}.

Using singlet depletion method,[45] the triplet extinction coefficients (ε_T) of five PCBM-like fullerene derivatives are determined. With ε_T available, triplet state quantum yields (Φ_T) can be derived by the comparative method[46] using C_{60} as reference (Φ_T is known to be unity and ε_T = 20 200 M^{-1} cm^{-1}).[44] These values are summarized in Table 1. Obviously, the triplet state quantum yields (Φ_T) of the five PCBM-like fullerene derivatives are all reduced to almost one-half of that of C_{60}. The decreasing of triplet state quantum yields corroborates the enhanced fluorescence yields. Both phenomena can be ascribed to the symmetry breaking effect of functional groups adducted to the C_{60} core, which perturbs the forbidden transitions from S_1 to S_0 state. While the transition probabilities from S_1 to S_0 state are enhanced, the populations branched to T_1 state by intersystem crossing ($S_1 \rightarrow T_1$) are decreased accordingly, resulting in significantly decreased triplet quantum yields for the five fullerene derivatives as compared to that of C_{60}. On the other hand, increasing of the side chain length affects little the triplet spectra and quantum yields, and no significant differences exist among the five PCBM-like fullerene derivatives, as shown in Figure 2 and Table 1.

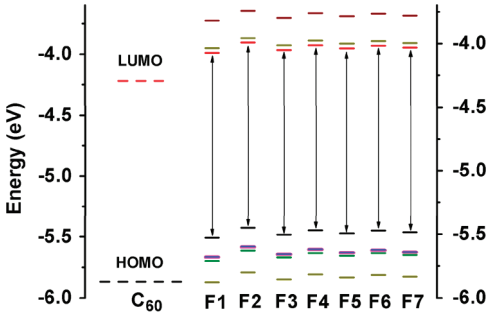

Figure 3. Energy levels of C_{60} and its derivatives calculated at the PBEPBE/6-311G(d,p) level. C_{60} has 5-fold degenerated HOMOs and 3-fold degenerated LUMOs, while the related energy levels for fullerene derivatives become nondegenerated. The HOMO and LUMO levels for the fullerene derivatives are denoted with arrow lines.

Summarizing the spectral data, our findings confirm that functionalization of a C═C double bond basically perturbs the

dx.doi.org/10.1021/jp208520v |J. Phys. Chem. A 2012, 116, 255–262

Table 2. Bond Lengths, HOMO Energy, LUMO Energy, and HOMO−LUMO E_{gap} of C_{60} Calculated with B3LYP and PBE Functionals, Respectively

	expt.	B3LYP/ 6-311G(d,p)	PBEPBE/ 6-311G(d,p)
HOMO/eV	−6.1[a,b]	−6.402	−5.870
LUMO/eV	−4.3[a,b]	−3.658	−4.220
E_{gap}/eV	1.57[c,d]−1.8[a,b]	2.743	1.650
	1.458(6)[e]		
C5−5/Å	1.455[f]	1.4539	1.4574
	1.45 ± 0.015[g]		
	1.401(1)[e]		
C6−6/Å	1.391[f]	1.3951	1.4041
	1.40 ± 0.015[g]		

[a] Cited from ref 54. [b] Cited from ref 55. [c] Cited from ref 52. [d] Cited from ref 53. [e] Cited from ref 56. [f] Cited from ref 57. [g] Cited from ref 58.

fullerene's π-system and breaks the I_h symmetry of pristine C_{60}, which results in modifications of photophysical properties of the five PCBM-like fullerene derivatives. Meanwhile, increasing the CH_2 chain length on the functional groups induces little changes among five derivatives. On the other hand, previous work[35] found that different photovoltaic performances were displayed among the five PCBM-like fullerene derivatives. How are these differences in photovoltaic performances originated?

Intrinsically, electronic properties are important factors affecting the photovoltaic performance of fullerene derivatives in PSCs. On one hand, the difference between the LUMO energy of an acceptor fullerene derivative and the HOMO energy of a donor polymer determines the upper limit of open circuit voltage (V_{oc}) of the PSC.[47,48] On the other hand, the overall energetic driving force for electron transfer from the donor to the acceptor is represented by the energy difference between the LUMOs of the donor and acceptor. An energy of 0.3−0.5 eV for LUMO(D)−LUMO(A) is necessary for efficient charge generation, while too large of a LUMO(D)−LUMO(A) gap will result in a waste of energy.[49,50] Therefore, raising the LUMO level of the acceptor takes the advantage increasing V_{oc} of PSCs. For this reason, we performed electronic structure calculations to examine the LUMO levels of the five PCBM-like fullerene derivatives and their expected influence on the photovoltaic performance.

Stable geometrical structures of the five fullerene derivatives and C_{60} were optimized with the Gaussian 03 program at the PBEPBE/6-31G(d) level. Orbital energy calculations and orbital analysis were performed at the higher level of PBEPBE/6-311G(d,p) using the optimized geometries. The calculated HOMO and LUMO energy levels are depicted in Figure 3.

PBE functional has been proved to yield reliable results for fullerene systems,[51] while the most commonly used B3LYP functional performs rather poorly. Table 2 presents a comparison of the HOMO and LUMO energies, HOMO−LUMO gap, and bond length for C_{60} obtained from B3LYP and PBE functional, respectively. Each parameter obtained from PBE functional agrees well with experimental results, while B3LYP functional yields a HOMO−LUMO gap of 2.743 eV that is largely deviating from the experimental value of 1.57−1.8 eV.[52−55] Therefore, PBE is an appropriate functional for describing the electronic structures of fullerene and its derivatives and has been adopted in our calculation.

Table 3. LUMO Energy and HOMO−LUMO Energy Gap (E_{gap}) for F1, F2, F3, F4, F5, F6, F7, and C_{60} Obtained with the PBEPBE/6-311G(d,p) Calculations, along with the Predicted Open Circuit Voltages V_{oc}[a]

			LUMO/eV		V_{oc}/V	
samples	symm.	E_{gap}/eV	expt.	calc.	expt.	calc.
F1	C_1	1.456	−3.91[b]	−4.074	0.564[b]	0.526
F2	C_1	1.458	−3.91[b]	−3.992	0.571[b]	0.608
F3	C_1	1.452	−3.92[b]	−4.052	0.535[b]	0.548
F4	C_1	1.458	−3.90[b]	−4.013	0.596[b]	0.587
F5	C_1	1.455	−3.91[b]	−4.038	0.540[b]	0.562
F6	C_1	1.454		−4.018		0.582
F7	C_1	1.452		−4.033		0.567
C_{60}	I_h	1.650	−4.3[c]	−4.220		

[a] All data are compared to the experimental results if available. [b] Data cited from ref 35. [c] Data cited from refs 54 and 55.

Table 3 displays the electronic structure calculation results for the five PCBM-like fullerene derivatives and their reference C_{60}. The calculated HOMO−LUMO energy gap is 1.65 eV for C_{60}, while it reduced to ∼1.46 eV for the five fullerene derivatives. The calculated LUMO energies for the five derivatives are all raised to ∼ −4.0 eV, as compared to that of C_{60} (∼ −4.2 eV). In general, the calculated orbital energies agree with those determined from experimental measurements[35] with approximately 0.1 eV of deviation, which is reasonable for large carbon systems.

Heeger and co-workers reported an empirical equation to estimate the open circuit voltage V_{oc} by fitting 26 different BHJ solar cells,[48] shown as the following:

$$V_{oc} = (1/e)(|E_{HOMO}^{donor}| - |E_{LUMO}^{acceptor}|) - 0.3\ V$$

where e is the elementary charge and 0.3 V is an empirical factor. Using this equation and the calculated LUMO energies, the V_{oc} values can be predicted for the PSCs with P3HT as donor and F1−F5 as acceptors, as listed in Table 3. The HOMO energy of the donor P3HT, −4.9 eV, is cited from experimental measurements by ultraviolet photoelectron spectroscopy.[59] Basically, the calculated V_{oc} values agree with the experimental data, in their variation trend from F1 to F5. Instead of a monotonic variation, the amplitude of V_{oc} oscillates with the CH_2 chain length of F1−F5, showing larger values for F2 and F4, but smaller values for F1, F3, and F5, for both the experimental and the calculation data. As compared to the experimental data, the calculation data exhibit this trend more clearly. Where does this variation trend of V_{oc} result from?

In BHJ solar cells, the energy difference between the LUMO of a given fullerene derivative and the HOMO of a donor polymer determines the upper limit of V_{oc}, as explicitly expressed in the above empirical equation. With P3HT as the common donor, raising the acceptor's LUMO level is a dominant way to increase the V_{oc}. For the five fullerene derivatives, the calculated LUMO energies do not vary monotonically from F1 to F5, but rather display higher values for F2 and F4, and lower values for F1, F3, and F5, as shown in Figure 3 and Table 3. As a result, F2 and F4 display higher V_{oc} values as compared to those of F1, F3, and F5. Such an oscillating trend of V_{oc} is basically caused by the oscillation of LUMO energies from F1 to F5, according to our electronic structure calculations. On the other hand, as shown in Table 3, although the experimentally measured V_{oc} values[35]

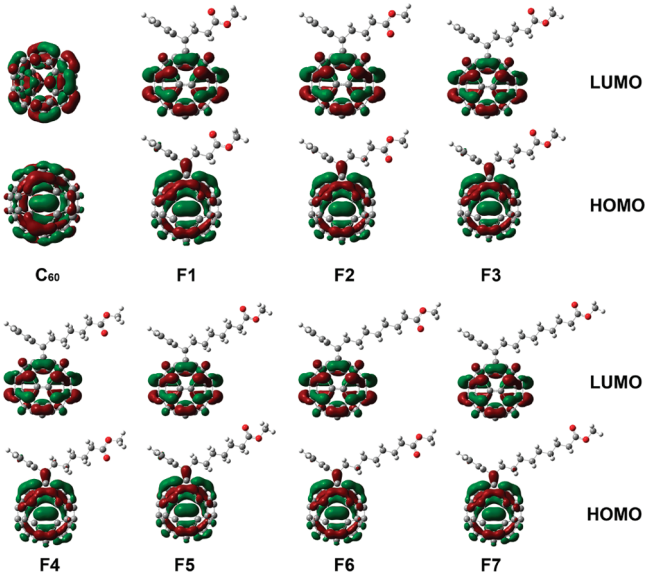

Figure 4. HOMO and LUMO orbitals for C_{60} and the fullerene derivatives obtained with the PBEPBE/6-311G(d,p) calculations.

exhibit an oscillating trend from F1 to F5, the LUMO energies determined from cyclic voltammetry experiments[35] are almost identical to each other (~ -3.9 eV). In contrast to this discrepancy between experimental measurements, our electronic structure calculations afford reasonable explanations because it reveals the small variation of LUMO energies, whereas the cyclic voltammetry experiments[35] failed. More accurate methods, such as ultraviolet photoelectron spectroscopy, are required to determine these LUMO energies experimentally.

PBEPBE/6-311G(d,p) level of orbital analysis was performed to understand the modified electronic properties for the five PCBM-like fullerene derivatives relative to C_{60}. The HOMO and LUMO orbitals obtained with the PBE functional are depicted in Figure 4. The five fullerene derivatives have very similar molecular structures, with the functional groups fused to the fullerene core through one cyclopropane ring. Such a similarity in molecular structures, as a result, leads to similar electronic properties. As compared to the pristine C_{60}, the HOMO and LUMO orbitals for the five fullerene derivatives become less diffusively spread, as shown in Figure 4. For LUMOs, nodal planes emerge in the middle of the C_{60} core, which appears to limit the electron delocalization to two separate parts, the upper and lower parts of C_{60}. As a result, the electron delocalization becomes less strong, and thus the LUMO energy levels are raised markedly for the five fullerene derivatives relative to the pristine C_{60}. In fact, this weakened electron delocalization is consistent with the contraction of π-system caused by C═C bond functionalization. Both effects lead to a raise of LUMO levels for fullerene derivatives.

Why does the amplitude of the LUMO energies oscillate from F1 to F5, instead of varying monotonically as the CH_2 chain of the functional group lengthened from F1 to F5? For the five fullerene derivatives, the HOMOs and LUMOs present almost the same orbital distribution with the majority of the electron densities being located on the C_{60} core and nearly no distribution on side chain functional groups. However, the side chain functional groups of $-COOCH_3$ induce great electron-withdrawing effect, as manifested by the shift of HOMO electron densities to the top C_{60} core where the functional groups are adducted (see Figure 4). Such an electron-withdrawing effect might perturb the LUMO energies subtly; that is, when the side chain carbonyl group adopts a cis conformation relative to the C_{60} core in the case of F2 and F4 (see Scheme 1), the electron-withdrawing effect tends to become greater than that of the case for F1, F3, and F5 with a trans conformation, and, as a result, F2 and F4 display higher LUMO energies than those of F1, F3, and F5. This postulation can be testified by extending the electronic structure calculations to longer CH_2 chain fullerene derivatives, F6 and F7. As shown in Table 3 and Figure 3, F6 with a cis conformation displays higher LUMO energy level than that of F7 with a trans conformation. In addition, the oscillating trend of the LUMO energies with the CH_2 chain length becomes less obvious when the electron -withdrawing group $-COOCH_3$ lies further apart from the C_{60} core from F1 to F7, which corroborates the postulation that the oscillating trend is induced by the electron-withdrawing effect of functional groups.

4. CONCLUSION

For the five PCBM-like C_{60} derivatives (F1, F2, F3, F4, and F5), we have characterized their photophysical and electronic properties that are crucial factors affecting the photovoltaic performance of PSCs. The transient UV−visible absorption spectra, transient fluorescence decay, together with the steady-state UV−visible absorption and fluorescence spectra were measured, showing that the fluorescence quantum yields (Φ_F) are enhanced and the triplet quantum yields (Φ_T) are lowered for the five PCBM-like C_{60} derivatives as compared to those of the pristine C_{60}. These spectral features confirm that functionalization of a C═C double bond perturbs the fullerene's π-system and breaks the I_h symmetry of pristine C_{60}, which results in modifications of photophysical properties of the fullerene derivatives. The significantly lowered triplet quantum yields for the five PCBM-like C_{60} derivatives, as compared to C_{60}, render these molecules better acceptor materials in PSCs, by preventing the triplet exciton formation that could lead to energy losses.

Electronic structure calculations were performed to obtain the HOMO−LUMO gaps and LUMO energies with the PBEPBE/6-311G(d,p)//PBEPBE/6-31G(d) level of density functional theories. Using the calculated LUMO energies and Heeger's empirical equation, the open circuit voltage V_{oc} values were predicted for the PSCs with P3HT as donor and F1−F5 as acceptors. As compared to the pristine C_{60}, the five fullerene derivatives display raised LUMO energy levels, from which larger open circuit voltages V_{oc} are resulted. Among the five fullerene derivatives, the amplitude of LUMO energies does not vary monotonically from F1 to F5 as the CH_2 chain lengthens, but rather displays an oscillating trend, which results in larger V_{oc} values for F2 and F4, and smaller V_{oc} values for F1, F3, and F5. The predicted V_{oc} values from our calculations agree with previous experimental results[35] and afford reasonable explanations by revealing the small variation of LUMO energies. The Orbital analysis indicates that the oscillating trend of LUMO energy levels and V_{oc} values could be induced by the electron-withdrawing effect of side functional groups, which tends to become stronger in the case of F2 and F4 when the side chain carbonyl group adopts a cis conformation relative to the C_{60} core, than that of the case for F1, F3, and F5 with a trans conformation.

Basically, functionalization of a C═C double bond sustains the fullerene structure and thus its electron affinitive properties. Adducted side chains result in little changes for the photophysical

properties among the five PCBM-like fullerene derivatives, but contribute to improve the compatibility of the polymer/fullerene system as well as adjust the HOMO−LUMO gap and LUMO levels of the acceptors to improve open circuit voltage in polymer photovoltaics. The results provide insights for understanding how structural modifications of functionalization influence the photovoltaic performance.

AUTHOR INFORMATION

Corresponding Author

*E-mail: hongmei@iccas.ac.cn.

ACKNOWLEDGMENT

This work was financially supported by the National Natural Science Foundation of China (Grant nos. 20733005, 20973179, and 21073201) and the Chinese Academy of Sciences. We would like to thank Prof. Andong Xia for discussions and use of the TCSPC spectrometer.

REFERENCES

(1) Yu, G.; Gao, J.; Hummelen, J. C.; Wudl, F.; Heeger, A. J. *Science* **1995**, *270*, 1789–1791.
(2) Shaheen, S. E.; Brabec, C. J.; Sariciftci, N. S.; Padinger, F.; Fromherz, T.; Hummelen, J. C. *Appl. Phys. Lett.* **2001**, *78*, 841–843.
(3) Kroon, J. M.; Wienk, M. M.; Verhees, W. J. H.; Hummelen, J. C. *Thin Solid Films* **2002**, *403*, 223–228.
(4) Svensson, M.; Zhang, F. L.; Veenstra, S. C.; Verhees, W. J. H.; Hummelen, J. C.; Kroon, J. M.; Inganas, O.; Andersson, M. R. *Adv. Mater.* **2003**, *15*, 988–991.
(5) Kim, J. Y.; Kim, S. H.; Lee, H. H.; Lee, K.; Ma, W. L.; Gong, X.; Heeger, A. J. *Adv. Mater.* **2006**, *18*, 572–576.
(6) Peet, J.; Kim, J. Y.; Coates, N. E.; Ma, W. L.; Moses, D.; Heeger, A. J.; Bazan, G. C. *Nat. Mater.* **2007**, *6*, 497–500.
(7) Kim, J. Y.; Lee, K.; Coates, N. E.; Moses, D.; Nguyen, T. Q.; Dante, M.; Heeger, A. J. *Science* **2007**, *317*, 222–225.
(8) Sariciftci, N. S.; Smilowitz, L.; Heeger, A. J.; Wudl, F. *Science* **1992**, *258*, 1474–1476.
(9) Hummelen, J. C.; Knight, B. W.; Lepeq, F.; Wudl, F.; Yao, J.; Wilkins, C. L. *J. Org. Chem.* **1995**, *60*, 532–538.
(10) Thompson, B. C.; Frechet, J. M. J. *Angew. Chem., Int. Ed.* **2008**, *47*, 58–77.
(11) Peet, J.; Heeger, A. J.; Bazan, G. C. *Acc. Chem. Res.* **2009**, *42*, 1700–1708.
(12) Brabec, C. J.; Gowrisanker, S.; Halls, J. J. M.; Laird, D.; Jia, S. J.; Williams, S. P. *Adv. Mater.* **2010**, *22*, 3839–3856.
(13) He, Y. J.; Li, Y. F. *Phys. Chem. Chem. Phys.* **2011**, *13*, 1970–1983.
(14) Padinger, F.; Rittberger, R. S.; Sariciftci, N. S. *Adv. Funct. Mater.* **2003**, *13*, 85–88.
(15) Li, G.; Shrotriya, V.; Huang, J. S.; Yao, Y.; Moriarty, T.; Emery, K.; Yang, Y. *Nat. Mater.* **2005**, *4*, 864–868.
(16) Ma, W. L.; Yang, C. Y.; Gong, X.; Lee, K.; Heeger, A. J. *Adv. Funct. Mater.* **2005**, *15*, 1617–1622.
(17) Kim, Y.; Cook, S.; Tuladhar, S. M.; Choulis, S. A.; Nelson, J.; Durrant, J. R.; Bradley, D. D. C.; Giles, M.; McCulloch, I.; Ha, C. S.; Ree, M. *Nat. Mater.* **2006**, *5*, 197–203.
(18) Guldi, D. M.; Asmus, K. D. *J. Phys. Chem. A* **1997**, *101*, 1472–1481.
(19) Ma, B.; Bunker, C. E.; Guduru, R.; Zhang, X. F.; Sun, Y. P. *J. Phys. Chem. A* **1997**, *101*, 5626–5632.
(20) Bensasson, R. V.; Bienvenue, E.; Fabre, C.; Janot, J. M.; Land, E. J.; Leach, S.; Leboulaire, V.; Rassat, A.; Roux, S.; Seta, P. *Chem.-Eur. J.* **1998**, *4*, 270–278.
(21) Luo, C.; Fujitsuka, M.; Watanabe, A.; Ito, O.; Gan, L.; Huang, Y.; Huang, C. H. *J. Chem. Soc., Faraday Trans.* **1998**, *94*, 527–532.
(22) Sun, Y. P.; Guduru, R.; Lawson, G. E.; Mullins, J. E.; Guo, Z. X.; Quinlan, J.; Bunker, C. E.; Gord, J. R. *J. Phys. Chem. B* **2000**, *104*, 4625–4632.
(23) Zheng, L. P.; Zhou, Q. M.; Deng, X. Y.; Yuan, M.; Yu, G.; Cao, Y. *J. Phys. Chem. B* **2004**, *108*, 11921–11926.
(24) Troshin, P. A.; Hoppe, H.; Renz, J.; Egginger, M.; Mayorova, J. Y.; Goryochev, A. E.; Peregudov, A. S.; Lyubovskaya, R. N.; Gobsch, G.; Sariciftci, N. S.; Razumov, V. F. *Adv. Funct. Mater.* **2009**, *19*, 779–788.
(25) Lenes, M.; Wetzelaer, G.; Kooistra, F. B.; Veenstra, S. C.; Hummelen, J. C.; Blom, P. W. M. *Adv. Mater.* **2008**, *20*, 2116–2119.
(26) Lenes, M.; Shelton, S. W.; Sieval, A. B.; Kronholm, D. F.; Hummelen, J. C.; Blom, P. W. M. *Adv. Funct. Mater.* **2009**, *19*, 3002–3007.
(27) Choi, J. H.; Son, K. I.; Kim, T.; Kim, K.; Ohkubo, K.; Fukuzumi, S. *J. Mater. Chem.* **2010**, *20*, 475–482.
(28) Kooistra, F. B.; Knol, J.; Kastenberg, F.; Popescu, L. M.; Verhees, W. J. H.; Kroon, J. M.; Hummelen, J. C. *Org. Lett.* **2007**, *9*, 551–554.
(29) Yang, C.; Kim, J. Y.; Cho, S.; Lee, J. K.; Heeger, A. J.; Wudl, F. *J. Am. Chem. Soc.* **2008**, *130*, 6444–6450.
(30) Zhang, Y.; Yip, H. L.; Acton, O.; Hau, S. K.; Huang, F.; Jen, A. K. Y. *Chem. Mater.* **2009**, *21*, 2598–2600.
(31) He, Y. J.; Chen, H. Y.; Hou, J. H.; Li, Y. F. *J. Am. Chem. Soc.* **2010**, *132*, 1377–1382.
(32) Zhao, G. J.; He, Y. J.; Li, Y. F. *Adv. Mater.* **2010**, *22*, 4355–4358.
(33) Ross, R. B.; Cardona, C. M.; Guldi, D. M.; Sankaranarayanan, S. G.; Reese, M. O.; Kopidakis, N.; Peet, J.; Walker, B.; Bazan, G. C.; Van Keuren, E.; Holloway, B. C.; Drees, M. *Nat. Mater.* **2009**, *8*, 208–212.
(34) Ross, R. B.; Cardona, C. M.; Swain, F. B.; Guldi, D. M.; Sankaranarayanan, S. G.; Van Keuren, E.; Holloway, B. C.; Drees, M. *Adv. Funct. Mater.* **2009**, *19*, 2332–2337.
(35) Zhao, G. J.; He, Y. J.; Xu, Z.; Hou, J. H.; Zhang, M. J.; Min, J.; Chen, H. Y.; Ye, M. F.; Hong, Z. R.; Yang, Y.; Li, Y. F. *Adv. Funct. Mater.* **2010**, *20*, 1480–1487.
(36) Schueppel, R.; Schmidt, K.; Uhrich, C.; Schulze, K.; Wynands, D.; Bredas, J. L.; Brier, E.; Reinold, E.; Bu, H. B.; Baeuerle, P.; Maennig, B.; Pfeiffer, M.; Leo, K. *Phys. Rev. B* **2008**, *77*, 085311.
(37) Wang, H.; Su, H. M.; Qian, H. L.; Wang, Z. H.; Wang, X. F.; Xia, A. D. *J. Phys. Chem. A* **2010**, *114*, 9130–9135.
(38) Perdew, J. P.; Burke, K.; Ernzerhof, M. *Phys. Rev. Lett.* **1996**, *77*, 3865–3868.
(39) Frisch, M. J.; et al. *Gaussian 03*, revision E.01; Gaussian, Inc.: Wallingford, CT, 2004.
(40) Lin, S. K.; Shiu, L. L.; Chien, K. M.; Luh, T. Y.; Lin, T. I. *J. Phys. Chem.* **1995**, *99*, 105–111.
(41) Kim, D.; Lee, M.; Suh, Y. D.; Kim, S. K. *J. Am. Chem. Soc.* **1992**, *114*, 4429–4430.
(42) Williams, R. M.; Zwier, J. M.; Verhoeven, J. W. *J. Am. Chem. Soc.* **1995**, *117*, 4093–4099.
(43) Dimitrijevic, N. M.; Kamat, P. V. *J. Phys. Chem.* **1992**, *96*, 4811–4814.
(44) Bensasson, R. V.; Hill, T.; Lambert, C.; Land, E. J.; Leach, S.; Truscott, T. G. *Chem. Phys. Lett.* **1993**, *201*, 326–335.
(45) Carmichael, I.; Hug, G. L. *J. Phys. Chem. Ref. Data* **1986**, *15*, 1–250.
(46) Bensasson, R. V.; Bienvenue, E.; Janot, J. M.; Leach, S.; Seta, P.; Schuster, D. I.; Wilson, S. R.; Zhao, H. *Chem. Phys. Lett.* **1995**, *245*, 566–570.
(47) Brabec, C. J.; Cravino, A.; Meissner, D.; Sariciftci, N. S.; Fromherz, T.; Rispens, M. T.; Sanchez, L.; Hummelen, J. C. *Adv. Funct. Mater.* **2001**, *11*, 374–380.
(48) Scharber, M. C.; Wuhlbacher, D.; Koppe, M.; Denk, P.; Waldauf, C.; Heeger, A. J.; Brabec, C. L. *Adv. Mater.* **2006**, *18*, 789–794.
(49) Halls, J. J. M.; Cornil, J.; dos Santos, D. A.; Silbey, R.; Hwang, D. H.; Holmes, A. B.; Bredas, J. L.; Friend, R. H. *Phys. Rev. B* **1999**, *60*, 5721–5727.
(50) Koster, L. J. A.; Mihailetchi, V. D.; Blom, P. W. M. *Appl. Phys. Lett.* **2006**, *88*, 093511.
(51) Beu, T. A.; Onoe, J.; Hida, A. *Phys. Rev. B* **2005**, *72*, 155416.

(52) Wang, X. B.; Ding, C. F.; Wang, L. S. *J. Chem. Phys.* **1999**, *110*, 8217–8220.
(53) Li, J.; Li, X.; Zhai, H. J.; Wang, L. S. *Science* **2003**, *299*, 864–867.
(54) Allemand, P. M.; Koch, A.; Wudl, F.; Rubin, Y.; Diederich, F.; Alvarez, M. M.; Anz, S. J.; Whetten, R. L. *J. Am. Chem. Soc.* **1991**, *113*, 1050–1051.
(55) Koeppe, R.; Sariciftci, N. S. *Photochem. Photobiol. Sci.* **2006**, *5*, 1122–1131.
(56) Hedberg, K.; Hedberg, L.; Bethune, D. S.; Brown, C. A.; Dorn, H. C.; Johnson, R. D.; Devries, M. *Science* **1991**, *254*, 410–412.
(57) David, W. I. F.; Ibberson, R. M.; Matthewman, J. C.; Prassides, K.; Dennis, T. J. S.; Hare, J. P.; Kroto, H. W.; Taylor, R.; Walton, D. R. M. *Nature* **1991**, *353*, 147–149.
(58) Yannoni, C. S.; Bernier, P. P.; Bethune, D. S.; Meijer, G.; Salem, J. R. *J. Am. Chem. Soc.* **1991**, *113*, 3190–3192.
(59) Gong, X.; Tong, M. H.; Brunetti, F. G.; Seo, J.; Sun, Y. M.; Moses, D.; Wudl, F.; Heeger, A. J. *Adv. Mater.* **2011**, *23*, 2272–2277.